These days, during the issues of climate change, there has been a shift in the energy industry from using fossil fuels to more environmentally friendly fuels such as biomass fuels. Biomass fuel is considered CO_2 neutral because the carbon produced during combustion in the form of CO_2 emissions can be used for new plant growth. However, besides the advantages of using biomass fuel, a problem arises when biomass fuel contains a high concentration of corrosive agents, which can be released along with hot fuel gas. These corrosive agents can damage the boiler components. Coating technology is one of the solutions to protect components that work at high temperatures against the corrosion threat. One type of coating that can be used in high-temperature applications is NiCrAlY coating by the high-velocity oxide (HVOF) process. One interesting topic that people are developing is using nano-scale coating to increase the coating's resistance against hot corrosion and cracking. Nano-scale powder feedstock is needed to produce nano-scale coating material. In this research, top-down method is used to synthesis nano-scale powder. One of top down method, the high-energy ball milling processs, is a promising method to synthesize nano-scale powder material. Therefore, in this research, the ball milling process is used to prepare nano-scale product. The results showed that this method was successful to make the nano-scale powder. The nano-scale powder was characterized by several methods to investigate the morphology and properties of the powders. However, there are still many challenges in producing nano-scale powder that meets HVOF feedstock powder requirements. In the long run, it is expected that this research can answer those challenges so that at the end, the good quality of nano-scale powder can be achieved

Keywords: coating, high-velocity oxygen fuel (HVOF), NiCrAlY, nano-scale powder, high-energy ball milling

UDC 620
DOI: 10.15587/1729-4061.2024.307040

SYNTHESIS OF NICrAlY NANO-SCALE POWDER BY HIGH-ENERGY BALL MILLING PROCESS FOR THERMAL SPRAY COATING APPLICATION

Irma Pratiwi
Corresponding author
Doctoral Student of Materials Engineering Program*
E-mail: irma031.ip@gmail.com
Husaini Ardy
Professor of Materials Engineering*
Budi Prawara
Head of Electronics and
Informatics Research Organization (BRIN)
National Research and Innovation Agency
Sangkuriang str., Bandung, Indonesia, 40135
Raden Dadan Ramdan
Lecturer of Materials Engineering*
Fahdzi Muttaqien
Lecturer of Computational Science
Department of Physics**
*Department of Materials Science and Engineering**
**Institut Teknologi Bandung
Ganesa str., 10, Bandung, Indonesia, 40132

Received date 25.03.2024
Accepted date 03.06.2024
Published date 28.06.2024

How to Cite: *Pratiwi, I., Ardy, H., Prawara, B., Ramdan, R. D., Muttaqien, F. (2024). Synthesis of NiCrAlY nano-scale powder by high-energy ball milling process for thermal spray coating application. Eastern-European Journal of Enterprise Technologies, 3 (12 (129)), 56–61. https://doi.org/10.15587/1729-4061.2024.307040*

1. Introduction

80 % of energy generally produce from fuel, especially coal [1]. In recent years, the energy industry has experienced a shift from the use of fossil fuels to the use of biomass and waste fuels such as straw and municipal solid waste (MSW) to reduce CO_2 emissions [2]. Unlike fossil fuels, fuels from biomass can be considered as CO_2-neutral because the carbon produced from the combustion process in the form of CO_2 emissions can be used for new plant growth. However, biomass fuels contain a high concentration of corrosive substances such as chloride (Cl_2), hydrogen chloride (HCl), and alkaline chloride (KCl or NaCl), which can be released along with hot fuel gases and damage the boiler tube components [2].

Failures usually occur in equipment which operates at high temperatures in industrial power generations. Those failures are caused by combination of erosion and corrosion. The phenomenon of corrosion and erosion at high temperatures mainly occurs in the combustion chamber, on the surface of the superheater and economizer, fuel and air feeding, and ash removal systems [3].

Thermal cyclic operation is one of the conditions that trigger the oxidation of the material. This problem is often found in components above 500 °C temperature [4]. Oxidation is a deterioration phenomenon that predominates in the moving components at high temperatures [5]. Methods to reduce corrosion and erosion include design optimization, selection of material and thickness, and coating [3]. Coating technology effectively protects the substrate from oxidation without any changes in the base material properties. There were many coating methods that have been used to prepare high-temperature oxidation resistant material. In Indonesia, they are used conventional size powder to prepare high-temperature resistance coating material for boiler application. However, with the shift from the use of fossil fuels to the use of biomass and waste fuels, the conventional coating is not sufficient because the boiler environment will be more corrosive from the biomass fuel combustion. With the advancement of materials engineering, many

studies showed that there are many benefits from the utilization of nano-scale material. Therefore, researches devoted for obtaining nano-sized powder are relevant.

2. Literature Review and Problem Statement

MCrAl (M for Ni, Co) based coatings have been used for mechanical components in equipments that operate in in high temperature and have high oxidation resistance and excellent mechanical properties. One of example, NiCoCrAlY-Ta coating, was used in the research by Yang et al. where Arc Ion Plating method was used to produce high-temperature oxidation resistance coating with the addition of vacuum heat treatment for better adhesion. However, after 200 h of oxidation at 1050 °C, cracks were found at Al_2O_3 layer [6].

Increasing oxidation resistance can be done as well by making a composite coating. [7] synthesized CoCrAlY-TiB_2 composite coating by air plasma spray (APS). The composite coating results had better bonding strength and oxidation resistance compare to single coating. However, the effect of powder size in the coating results were not studied in this research. The important factors that determine corrosion resistance of NiCoCrAlY coating are the size and distribution of the NiAl (β) phase [8]. However, the effect of nano-technology to the corrosion resistance of NiCrAlY based coating was not explained on this research.

The research about nano-technology for this application is still limited, especially in Indonesia. One study found that Alloy-718/NiCrAlY bi-layer coating exhibited lower oxidation rates due because it formed protective phases such as $NiCr_2O_4$, Al_2O_3, Cr_2O_3, and TiO_2 [4]. Meanwhile, in thermal barrier coating applications, (Ni, Co) CrAlY is usually applied in the bond coat that can convert Al to thermally grown oxide (TGO) alumina [9, 10]. Alumina is a protective layer that can resist oxidation at high temperatures due to its slow growth rate and thermodynamically stable [10]. Explanations regarding the mechanism of alumina corrosion protection in boiler coatings, both experimentally and modeling, are still limited.

Nanocoating is a thin layer in the dimensions of nanometers or nanoparticles that are dispersed and carry unique properties. There are four nanocoatings: nano-grade coatings, superlattice, and multi-layer coatings, thin-film coatings, and nanocomposite coatings [11]. Nano-composite coating is currently an interesting topic for further development. The physical thermomechanical properties of nano-coatings can be altered by controlling the structure, such as the size and distribution of the fully melted and partially melted of nano structured powder [12]. However, there are not many studies discussing the process of nano-coating powder synthesis.

A wide distribution of nano structure powder is needed to produce significant nano-structuring effects on coating. Currently, there are still many challenges in producing nanostructures in coating materials, especially in the powder synthesis process. Especially in Indonesia, there have not been many studies on nano-structure coatings for boilers. Even though boilers with biomass fuel which more corrosive are already used widely.

3. The aim and objectives of the study

The aim of this research is to achieve high quality nano-scale powder that meets HVOF feedstock powder requirements. With the high-quality nano-scale powder, the good quality nano-structure coating will be achieved.

To achieve this aim, the following objectives are determined:

– to conduct high-energy ball milling process (the top-down synthesis) with a certain parameter;

– to do several material characterizations on the ball-milled powder.

4. Materials and methods of research

4. 1. Object and hypothesis of the study

This research used Ni-22Cr-10Al-1Y (Amdry 962) powder with a size distribution of 45/10 μm. In the end, it is expected to achieved nano-scale powder by high energy ball milling process. Some assumptions and simplifications were made on this research as follows:

a) starting powder was assumed to be homogeneous;

b) ball milling process was assumed to be conduct in inert condition;

c) there was no significant temperature fluctuation during ball milling process;

d) ball milling process was assumed to be conduct in vacuum condition.

4. 2. Process for preparing nano-sized powder

The nano-scale Ni-22Cr-10Al-1Y powder was prepared by mechanical milling at room temperature in a high-energy planetary ball mill. The parameters of ball milling process can be seen on Table 1.

Table 1

Ball milling process parameter

Parameter	Value
Temperature (°C)	Room temperature as it is
Environment	Noble condition (controlled by argon gas)
Time total (hour)	36
Operating time (hour)	2
Off time (minute)	20
Rotating Cycle	18
Rotational speed (RPM)	96.67 and 322.22
Ball to powder ratio (wt%)	20:1
Sieving (mesh)	200

The milling vial was filled with high-purity argon and sealed to prevent oxidation. A process control agent (PCA) was added to avoid cold welding and bonding between the powder particles, between powder particles and the ball, and agglomeration during milling. The milling rotation speed was 96.67 and 322.22 rpm rotation with the ball-to-powder ratio (wt%) 20:1. Stearic acid synthetic grade was used as PCA. The milling time was 36 hours. After milling, the powder was sieved using a 200-mesh sieving apparatus.

4. 3. Methods for investigating the properties and characteristics of nano-sized powder

Visual observation was conducted on Ni-22Cr-10Al-1Y (Amdry 962) powder before and after the milling process to observe the powder's appearance. X-ray diffraction (XRD, Bruker D8 Advance) measurement was also con-

ducted to identify the phases in Ni-22Cr-10Al-1Y (Amdry 962) powder before and after the milling process. To observe the morphology and composition of powder before and after ball milling process, Scanning Electron Microscope (SEM, Hitachi SU3500) observation and Energy Dispersive Spectroscopy (EDS) measurement were conducted. Transmission Electron Microscope (TEM, Talos F200X) observation was conducted as well to observe the structure of Ni-22Cr-10Al-1Y (Amdry 962) powder after ball milling process.

5. Results of NiCrAlY nano-scale powder synthesis

5. 1. Results of high energy ball milling process

Fig. 1 shows as-milled powder in a ball mill vial. The ball-milled powder sticks around the alumina grinding ball.

a *b*

Fig. 1. The main signature: *a* — as-milled powder in ball mill vial for 96.67 rpm; *b* — as-milled powder in ball mill vial for 322.22 rpm

Fig. 2 shows a visual observation of as-milled powder. The color of the starting powder is light grey. The 96.67 rpm-ball milled powder shows a light grey color as well. However, the 322.22 rpm-ball milled powder shows a black color.

a *b* *c*

Fig. 2. The main signature: *a* — visual observation of starting powder; *b* — visual observation of as-milled powder 96.67 rpm; *c* — visual observation of as-milled powder 322.22 rpm

In this research, the wt% of PCA was varied to obtain the optimum PCA composition. The initial mass of powder and 1 wt% of PCA for one ball mill was 35.35 grams. The 96.67 rpm-ball mill process resulted in 34.757 grams of powder. Meanwhile, the 322.22 rpm ball mill process resulted in 35.44 grams of powder. The mass increases in 322.22 rpm-ball mill processed powder possibly came from the alumina grinding ball degradation. Table 2 shows the mass of powder resulting from several wt% of PCA.

The optimum wt% of PCA added to the powder was 1 wt%, which resulted in the highest ball mill efficiency (88.25 %).

Table 2

The percentage of PCA and powder yields

PCA composition (wt%)	Mass of starting powder+PCA (gram)	Powder yields (gram)	Efficiency (%)
1	35.35	31.195	88.25 %
3	36.05	23.738	65.84 %
4	36.40	26.197	71.97 %

5. 2. Powder characterization results

5. 2. 1. Scanning electron microscope characterization

Fig. 3 shows the morphology of starting powder NiCrAlY before the ball milling process and 96.67 rpm and 322.22 rpm ball milling process after 36 hours under a controlled atmosphere.

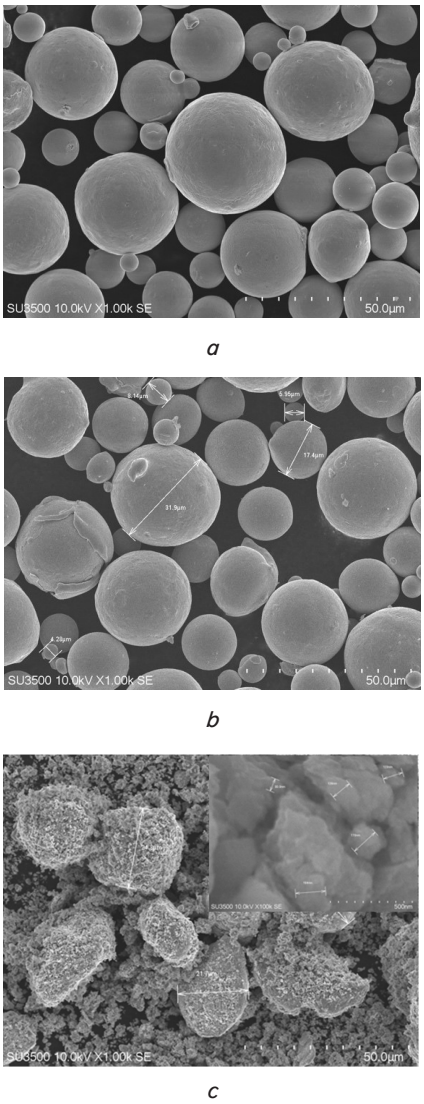

a

b

c

Fig. 3. The main signature: *a* — morphology of starting powder NiCrAlY; *b* — morphology of as-milled powder 96.67 rpm; *c* — morphology of as-milled powder 322.22 after 36 hours under a controlled atmosphere

NiCrAlY starting powder (a) showed a spherical shape with a smooth surface. 96.67 rpm ball milling process shows no significant effect on morphology change with the powder size range at 4.3 to 32 μm. However, 322.22 rpm ball milling resulted in semi-spherical agglomerate particles of 20 to

30 μm and consisted of nano-size powder with a flaky shape and rough surface.

5. 2. 2. X-Ray diffraction characterization

Based on the XRD pattern in Fig. 4, there was peak broadening in NiCrAlY powder after the 322.22 rpm ball milling process.

The starting powder shows sharp peaks consisting of Nickel Aluminide (Ni_3Al–γ'), Nickel-Cr Rich (γ), and NiAl (β). However, 322.22 rpm ball-milled powder shows only two broad peaks, (Ni_3Al–γ') and Nickel-Cr Rich (γ).

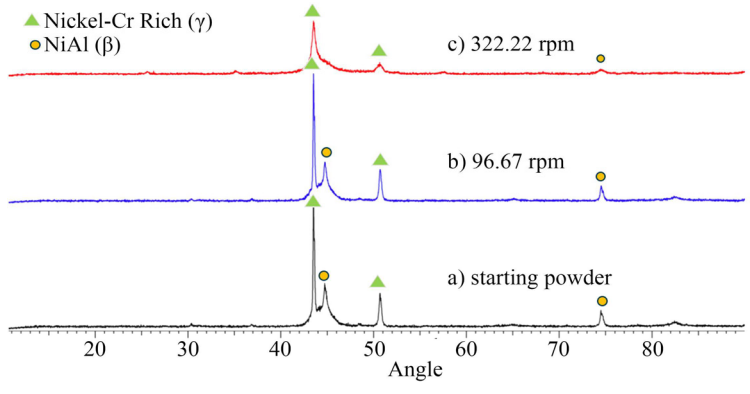

Fig. 4. The main signature: a — X-Ray diffraction peak of starting powder; b — 96.67 rpm ball-milled powder; c — 322.22 rpm ball-milled powder

5. 2. 3. Energy dispersive spectroscopy results

From the visual examination, a color change that observed at 322.22 rpm ball milled powder is suspected due to oxidation during ball milling process. Fig. 5 shows the EDS measurement of ball milled powder.

Based on the EDS measurement shown in Fig. 5, oxygen composition on 322.22 rpm ball-milled powder increases, which proves that oxidation occurred during ball milling.

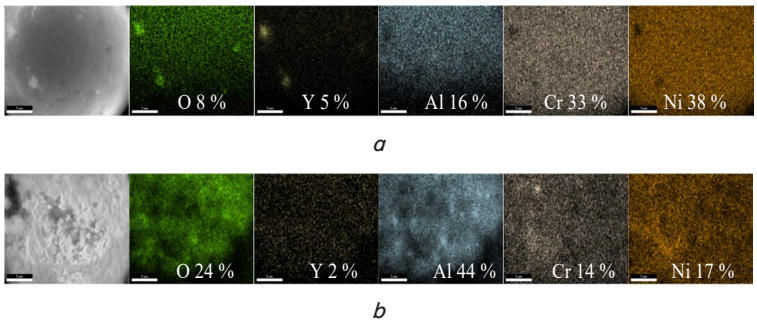

a

b

Fig. 5. The main signature: *a* — energy dispersive spectroscopy mapping of 96.67 rpm ball-milled powder; *b* — energy dispersive spectroscopy mapping of 322.22 rpm ball-milled powder

5. 2. 4. Transmission electron microscopy observation

Although XRD peaks indicate crystallite refinement, which can be calculated by measuring Bragg peak width at half of the maximum intensity, the overlaps in some peaks could result in incorrect grain size calculation results. Therefore, TEM observation was conducted. Fig. 6, *a* shows Transmission Electron Microscope (TEM) observation on one particle of 322.22 rpm ball-milled powder.

The range of particle size observed is 100–250 nm. Fig. 6, *b* shows that one powder particle consists of many small grains in different directions of atomic arrangements (red squares). This is the typical structure of polycrystalline material. However, these differences in atomic arrangements only can be captured clearly on some positions because the sample is relatively thick for TEM observation. In Fig. 6, *c*, the circular ring formation of the diffraction pattern indicates that the powder particle is polycrystalline. Using an image analyzer, based on Fig. 6, *b*, the average grain size of 322.22 rpm ball-milled powder is 7.82±2.88 nm.

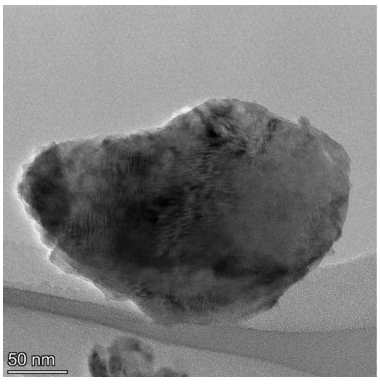

a

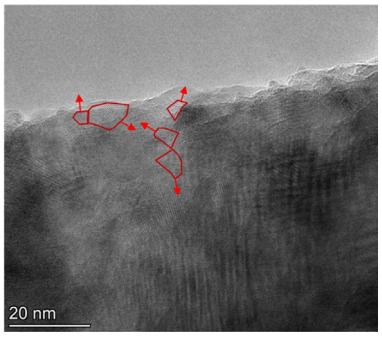

b

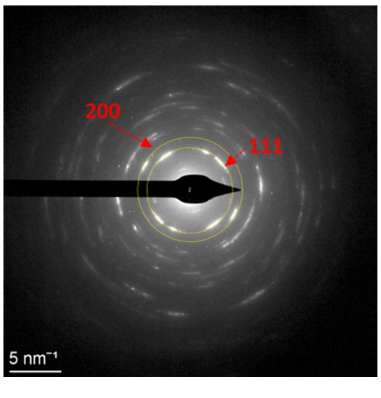

c

Fig. 6. The main signature: *a* — transmission electron microscope observation on one particle 322.22 rpm ball-milled powder; *b* — grain size of a powder particle; *c* — particle diffraction by transmission electron microscope observation

6. Discussions of the results: NiCrAlY nano-scale powder synthesis

From the Fig. 1, the smaller the particle size, the greater the surface area and van der Waals force, making it easier to

stick to the grinding ball surface. The higher the rotational speed of the ball mill, the higher the amount of powder sticks to the grinding ball and vial wall. For addition, in Fig. 2. There was color change on milled powder. The color change can occur due to oxidation during the milling.

From the Table 2, PCA was added to reduce the effect of cold welding by surface adsorbing mechanism during the ball milling [13]. The higher amount of PCA used in the ball milling process will reduce the particle size [13]. The smaller particle size tends to easily stick to the grinding ball or vial wall, resulting in lesser powder yields.

From the Fig. 3, fracturing and cold welding during the ball milling process caused the morphology to change, which led to agglomeration [13]. It is recommended that particle distribution for HVOF spraying is 5 to 45 μm. Therefore, both 96.67 and 322.22 rpm ball-milled powders meet the corresponding size requirement. However, only the 322.22 rpm ball milling that creates nano-sized powder. Therefore the 322.22 rpm is the optimum rotational speed to create nano-sized powder compare to 96.67 rpm.

Based on Fig. 4, Deformation during the ball milling process causes crystallite refinement and increases lattice strain. These two phenomena result in a peak broadening and a decrease in peak height [13]. Not only the broadening effect, (β) (NiAl) peak disappears, and the deviation of peaks. This finding also aligned with other similar research [14–17]. Al has a larger radius compared to Ni, which means that the dissolution of Al to γ phase will contribute to increased lattice parameters.

Based on the EDS measurement shown in Fig. 5, oxygen composition on 322.22 rpm ball-milled powder increases, which proves that oxidation occurred during ball milling. However, element composition measurement by EDS characterization should be used only for semi-quantitative analysis. Therefore, it needs other further characterization. Based on XRD peaks, no additional peak was detected on 322.22 rpm ball-milled powder, which means the possibility of oxidation during ball milling is low because no oxide peak was detected. Even if there was oxidation, the number of oxide phases formed during the ball milling process is relatively small which cannot be detected by XRD.

Based on transmission electron microscope observation, the circular ring formation of the diffraction pattern indicates that the powder particle is polycrystalline.

Based on the results above, nano-sized powder was successfully made by ball milling method. This nano-sized powder can be used as feeding powder to create nano-structure coating for high temperature application such as boiler tube. In the next step, high velocity oxy-fuel (HVOF) will be used to create this nano-structure coating that is predicted has higher corrosion resistance at high-temperature condition. Although the nano-scale powder is successfully made by ball-milling process in this research, there still some challenges in the morphology of milled powder which formed flaky and irregular shape. This irregular shape can affect flowability of powder during spraying process.

Therefore, another research regarding the improvement of the shape should be developed.

7. Conclusions

1. The color of the starting powder is light grey with indication of qualitative indicators of research results. The 96.67 rpm-ball milled powder color is still the same as the color of the original powder. However, the 322.22 rpm-ball milled powder color changed to black due to oxidation during milling. The optimum wt% of PCA added to the powder was 1 wt%, which resulted in the highest ball mill efficiency (88.25 %) with indication of quantitative indicators of research results.

2. Several characterizations have been conducted with results as follows:

a) NiCrAlY starting powder showed a spherical shape with a smooth surface. The shape did not change after milling at 96.67 rpm with the powder size range of 4.3 to 32 μm without nano-sized powder observed. However, 322.22 rpm ball milling resulted in semi-spherical agglomerate particles of 20 to 30 m and consisted of nano-size powder with a flaky shape and rough surface with indication of qualitative indicators of research results;

b) the XRD results show the peak broadening of NiCrAlY powder after the 322.22 rpm ball milling process due to severe plastic deformation during milling with indication of qualitative indicators of research results;

c) based on the EDS measurement, the oxygen composition on 322.22 rpm ball-milled powder increases, which proves that oxidation occurred during ball milling with indication of qualitative indicators of research results;

d) based on XRD peaks, no additional peak was detected on 322.22 rpm ball-milled powder, which means the possibility of oxidation during ball milling is low because no oxide peak was detected. Even if there was oxidation, the number of oxide phases formed during the ball milling process is relatively small which cannot be detected by XRD;

e) the particle size range observed is 100 to 250 nm. One powder particle has many small grain sizes in different directions of atomic arrangement. This is the typical structure of polycrystalline material. The circular ring formation of the diffraction pattern indicates that the powder particle is polycrystalline. The average grain size of 322.22 rpm ball-milled powder is 7.82±2.88 nm with indication of quantitative indicators of research results.

Conflict of interest

The authors declare that they have no conflict of interest in relation to this research, whether financial, personal, authorship or otherwise, that could affect the research and its results presented in this paper.

Financing

This research is supported by the Research, Community Services, and Innovation Program (PPMI) ITB 2023, Educational Fund Management Institution (LPDP) Ministry of Finance Indonesia, and National Research and Innovation Agency (BRIN).

Data availability

Data will be made available on reasonable request.

Use of artificial intelligence

The authors confirm that they did not use artificial intelligence technologies when creating the current work.

References

1. Wu, D., Yuan, Z., Liu, S., Zheng, J., Wei, X., Zhang, C. (2020). Recent Development of Corrosion Factors and Coating Applications in Biomass Firing Plants. Coatings, 10 (10), 1001. https://doi.org/10.3390/coatings10101001
2. Sadeghimeresht, E. (2018). Ni-based coatings for high temperature corrosion protection. University West. Available at: https://www.diva-portal.org/smash/get/diva2:1203387/FULLTEXT02.pdf
3. Szymański, K., Hernas, A., Moskal, G., Myalska, H. (2015). Thermally sprayed coatings resistant to erosion and corrosion for power plant boilers - A review. Surface and Coatings Technology, 268, 153–164. https://doi.org/10.1016/j.surfcoat.2014.10.046
4. Vasudev, H., Thakur, L., Bansal, A., Singh, H., Zafar, S. (2019). High temperature oxidation and erosion behaviour of HVOF sprayed bi-layer Alloy-718/NiCrAlY coating. Surface and Coatings Technology, 362, 366–380. https://doi.org/10.1016/j.surfcoat.2019.02.012
5. Lv, P., Sun, X., Cai, J., Zhang, C., Liu, X., Guan, Q. (2017). Microstructure and high temperature oxidation resistance of nickel based alloy GH4169 irradiated by high current pulsed electron beam. Surface and Coatings Technology, 309, 401–409. https://doi.org/10.1016/j.surfcoat.2016.11.041
6. Yang, H.-Z., Zou, J.-P., Shi, Q., Dai, M.-J., Lin, S.-S., Du, W., Lv, L. (2019). Analysis of the microstructural evolution and interface diffusion behavior of NiCoCrAlYTa coating in high temperature oxidation. Corrosion Science, 153, 162–169. https://doi.org/10.1016/j.corsci.2019.03.022
7. An, Q., Huang, L., Wei, S., Zhang, R., Rong, X., Wang, Y., Geng, L. (2019). Enhanced interfacial bonding and superior oxidation resistance of CoCrAlY-TiB_2 composite coating fabricated by air plasma spraying. Corrosion Science, 158, 108102. https://doi.org/10.1016/j.corsci.2019.108102
8. Luo, L., Zhang, H., Chen, Y., Zhao, C., Alavi, S., Guo, F. et al. (2018). Effects of the β phase size and shape on the oxidation behavior of NiCoCrAlY coating. Corrosion Science, 145, 262–270. https://doi.org/10.1016/j.corsci.2018.10.008
9. Quadakkers, W. J., Shemet, V., Sebold, D., Anton, R., Wessel, E., Singheiser, L. (2005). Oxidation characteristics of a platinized MCrAlY bond coat for TBC systems during cyclic oxidation at 1000 °C. Surface and Coatings Technology, 199 (1), 77–82. https://doi.org/10.1016/j.surfcoat.2004.11.038
10. Pint, B. A., More, K. L. (2009). Characterization of alumina interfaces in TBC systems. Journal of Materials Science, 44 (7), 1676–1686. https://doi.org/10.1007/s10853-008-3221-x
11. Shourgeshty, M., Aliofkhazraei, M., Alipour, M. M. (2016). Introduction to High-Temperature Coatings. High Temperature Corrosion. https://doi.org/10.5772/64282
12. Shi, P., Wang, W., Wan, S., Gao, Q., Sun, H., Feng, X. et al. (2021). Tribological performance and high temperature oxidation behaviour of thermal sprayed Ni- and NiCrAlY-based composite coatings. Surface and Coatings Technology, 405, 126615. https://doi.org/10.1016/j.surfcoat.2020.126615
13. Suryanarayana, C. (2001). Mechanical alloying and milling. Progress in Materials Science, 46 (1-2), 1–184. https://doi.org/10.1016/s0079-6425(99)00010-9
14. Zakeri, A., Bahmani, E., Aghdam, A. S. R. (2020). Impact of MCrAlY feedstock powder modification by high-energy ball milling on the microstructure and high-temperature oxidation performance of HVOF-sprayed coatings. Surface and Coatings Technology, 395, 125935. https://doi.org/10.1016/j.surfcoat.2020.125935
15. Khodsiani, Z., Mansuri, H., Mirian, T. (2013). The effect of cryomilling on the morphology and particle size distribution of the NiCoCrAlYSi powders with and without nano-sized alumina. Powder Technology, 245, 7–12. https://doi.org/10.1016/j.powtec.2013.04.010
16. Borchers, C., Stoltenhoff, T., Hahn, M., Schulze, M., Assadi, H., Suryanarayana, C. et al. (2014). Strain-Induced Phase Transformation of MCrAlY. Advanced Engineering Materials, 17 (5), 723–731. https://doi.org/10.1002/adem.201400174
17. Kaplin, C., Brochu, M. (2014). The effect of grain size on the oxidation of NiCoCrAlY. Applied Surface Science, 301, 258–263. https://doi.org/10.1016/j.apsusc.2014.02.056